ARTICLE

Synthesis, Anti-Cancer Screening and Molecular Docking of Saccharine-Triazole Hybrid Molecules using Copper(I) Catalyzed Click Chemistry

Kaushik D. Pambhar[1,✉], Vijay M. Khedkar[2], Vijay D. Chodvadiya[3], Ashish P. Dhamsaniya[1], Anamik K. Shah[4] and Ranjan C. Khunt[1]

Asian Pub. Corp.

www.asianpubs.org

Asian Journal of Organic & Medicinal Chemistry

Volume: 5 Year: 2020
Issue: 1 Month: January–March
pp: 68–76
DOI: https://doi.org/10.14233/ajomc.2020.AJOMC-P246

Received: 8 December 2019
Accepted: 6 March 2020
Published: 5 May 2020

ABSTRACT

Herein, we report the synthesis methodology and anticancer evaluation of 15 compounds using copper(I)-catalyzed azide alkyne cycloaddition (CuAAC) to develop a library of saccharin-1,2,3-triazole hybrid molecules. All library compounds showed interactions with various amino acids *via* the basic sulphonamide and amide linkage of the parental saccharin core motif. Molecular docking studies indicated that alternative positions of saccharin-1,2,3-triazole hybrid molecules added a diversity to the potential hydrogen bonding interactions of these compounds with various amino acids. Present results revealed that hybrid derivatives of saccharin which was prepared from saccharin azide was high yield using CuAAC approach. The compounds showed a moderate anti-cancer activity against SK-OV-3 ovarian cancer cell line and could be considered for the development of potential anticancer drugs based on these new molecules.

KEYWORDS

Saccharine, Substituted triazoles, Copper(I), Anti-cancer screening, Molecular docking, Click chemistry.

INTRODUCTION

The discovery of pharmaceutical lead candidate is very complex and challenging process as several methodologies involve in drug discovery or lead development but main disadvantage is that it take at least 12 to 15 years, despite among all approaches "hybrid molecules" concept reduce the time domain of lead expansion and increase the success rate of lead discovery, this strategy provide a wide variety of biologically active chemical space and diverse compounds library [1]. This strategy leads to the design of novel hybrid building blocks, which possess an individual therapeutics or possibility of new biologically activity. Various linkers like ester, amide, carbamate, sulfonamide, *etc*. generally used for a combination of heterocycles.

After the discovery of click chemistry, it become an efficient and rapid tool for regioselective synthesis of 1,2,3-triazole. Copper catalyzed click chemistry provided a high yield product within short duration [2,3]. Click chemistry is continuing growing and this methodology has shown by various applications in scientific area like synthesis of poly substituted1,2,3-

Author affiliations:

[1]Department of Chemistry, Saurashtra University, Rajkot-360005, India
[2]Department of Pharmaceutical Chemistry, Shri Vile Parle Kelavani Mandal's Institute of Pharmacy, Dhule-424001, India
[3]Faculty of Science, T.N. Rao College, Rajkot-360005, India
[4]Gujarat Vidhyapith, Ashram Road, Ahmedabad-380014, India

✉To whom correspondence to be addressed:

E-mail: rckhunt@sauuni.ac.in

Available online at: http://ajomc.asianpubs.org

trizole based bioconjugate [4], peptide, macromolecules like polymer and dendrimer [5,6], self-assembly, fluorescence probe [7], radiochemistry [8], *etc*.

Click chemistry is powerful template for synthesis of biologically active small triazole-heterocyclic hybrids. Among the all heterocycles, 1,2,3-triazole adduct generate a great interest because 1,2,3-triazole is a versatile moiety that spectacles various biological activities [9]. By presenting it into organic molecules, compounds with moderate dipole character, hydrogen bonding capability, rigidity and stability can be acquired [10]. So, the application of 1,2,3-triazole in pharmaceuticals and pesticides attracted more and more consideration. With the advance of contemporary heterocyclic chemistry, 1,2,3-triazole derivatives can be effortlessly synthesized through click chemistry reaction.

The saccharine containing molecules shows a broad spectrum of biological activities and have been used as inhibitors of histone deacetylase [11], tumor-associated carbonic anhydrase XII [12], kinase [13], human mast cell tryptase [14] and tyrosinase [15], α1a and α1c adrenergic receptor antagonists [16], anti-anxiety and antibacterial agents [17]. Moreover, saccharin is also found in many clinically used agents [18-20]. Recently, it is reported that *N*-formyl saccharin, a powerful formylating agent can be easily synthesized from saccharin, was used in formylation reaction [21,22].

Previous research on the biological screening of saccharin-1,2,3-triazole hybrids are limited (Fig. 1). To the best of our knowledge, the statistics of the biological activities of saccharin derivatives containing 1,2,3-triazole moiety have been rarely reported. Saccharine derivatives are less explored. So, present ongoing interest to construct a 1,2,3-triazole at nitrogen atom on saccharine by click transformation. In this study, a series of saccharin derivatives with 1,2,3-triazole moiety was synthesized and their anti-cancer activities were evaluated.

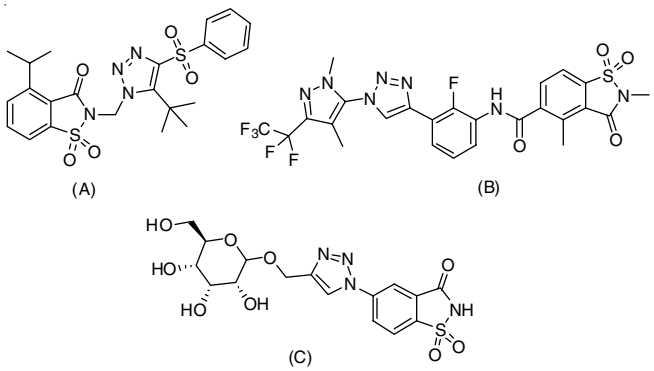

Fig. 1. Saccharine-triazole hybrids molecules

EXPERIMENTAL

All the solvents and reagents were obtained from Sigma-Aldrich and used without further purification. TLC for reaction monitoring using silica gel GF_{254} (Merck) plates. Melting points measured by open glass capillary method using digital melting point apparatus. IR spectra recorded on a Bruker IR spectrophotometer *via* KBr pallet method, proton, carbon spectrum was recorded on a Bruker AVANCE-III 400MHz spectrometer with 5 mm BBO probe head, TMS as internal reference. Mass (EI) spectra were recorded on a SHIMADZU QP-2010mass spectrometer.

Synthesis of 2-(prop-2-yn-1-yl)benzo[*d*]isothiazol-3-(2*H*)-one 1,1-dioxide (1a): In single-necked flat-bottomed flask was equipped with a Teflon-coated magnetic stir bar, saccharine (1 mmol) in DMF,was added K_2CO_3 (3 mmol) and 80% propargyl bromide in toluene (1.2 mmol) by dropwise manner and stirred the resulting mixture for 3 h at reflux temperature. The reaction was monitored by TLC (30% EtOAc:hexane). After completion of the reaction, the mixture was poured into ice-cold water with vigorous stirring. Filtered the mixture, washed with hexane and dried it to obtained pure product (**1a**). The product used further without purification (yield: 92%). m.p.: 188-190 ºC.

General procedure for the synthesis of 2-azido-*N*-substituted phenylacetamides (2a-o): To a solution of substituted aniline (5 mmol, 1 equiv.) in acetone and chloroacetyl chloride (5 mmol, 1 equiv.) was added by dropwise manner, a resulting mixture was stirred for 15 min at room temperature. Reaction mixture was then dumped onto crushed ice and solid intermediate product was precipitated out. Solid product was isolated by simple vacuum filtration, washed with hexane. The product used without further purification. Intermediate product (5 mmol) and NaN_3 (15 mmol) in DMF was stirred for 24 h at room temperature. After completion of reaction, mass was poured onto crushed ice and desired solid product (**2b**) was precipitated out. Filtered and washed with hexane to get desired product.

General procedure for derivatives of 2-(4-((1,1-dioxido-3-oxobenzo[I]isothiazol-2(3*H*)-yl)methyl)-1*H*-1,2,3-triazol-1-yl)-*N*-phenylacetamide (3a-o): An intermediate (**1**) (1 mmol) and **2** (1 mmol) were dissolved in 5 mL of a mixture of DMF:H_2O:*t*-BuOH (2:1:2). Sodium ascorbate (0.01 mmol) was added followed by $CuSO_4{\cdot}5H_2O$ (5 mol%) in water. The reaction mass was stirred continuously 4-5 h at room temperature. The reaction was monitor on TLC (10% MeOH:$CHCl_3$). After all starting materials were consumed on TLC, the reaction mass was quenched in saturated solution of NH_4Cl, cooled on ice and the precipitate was collected by filtration, washed with methanol (2 × 10 mL), dried it to afford pure product as solid powder (**3**) (**Scheme-I**).

Spectral data

***N*-(3-Chlorophenyl)-2-(4-((1,1-dioxido-3-oxobenzo[*d*]-isothiazol-2(3*H*)-yl)methyl)-1*H*-1,2,3-triazol-1-yl)acetamide (3a):** Off White solid, Yield: 85%, m.p.: 200 °C, R_f = 0.60, (10:90; MeOH:$CHCl_3$), ^{1}H NMR (400 MHz, DMSO-d_6) δ ppm: 10.29 (s, 1H), 8.10 (s, 1H), 8.03 (ddd, *J* = 7.4, 3.1, 1.6 Hz, 2H), 7.91 (td, *J* = 7.5, 1.4 Hz, 1H), 7.73 (t, *J* = 1.5 Hz, 1H), 7.52 (td, *J* = 7.5, 1.5 Hz, 1H), 7.45 (dt, *J* = 7.5, 1.5 Hz, 1H), 7.26 (t, *J* = 7.4 Hz, 1H), 7.04 (dt, *J* = 7.5, 1.5 Hz, 1H), 5.13 (s, 2H), 4.83 (d, *J* = 15.4 Hz, 1H), 4.47 (d, *J* = 15.2 Hz, 1H). ^{13}C NMR (100 MHz, DMSO) δ ppm: 168.77, 159.06, 141.39, 139.37, 138.47, 133.42, 133.34, 133.25, 132.90, 129.93, 126.03, 123.99, 123.92, 122.10, 121.04, 119.86, 52.53, 38.82. Mass (EI) calcd. for $C_{18}H_{14}N_5O_4SCl$ $[M+H]^+$ 431.52; found 431. IR (KBr, ν_{max}, cm^{-1}): 3252, 1728, 1718, 1678, 1626, 1552, 1456, 1411, 1367, 1298, 1261, 1230, 1160, 1111, 1053, 976, 883, 750, 667.

***N*-(2,6-Dimethylphenyl)-2-(4-((1,1-dioxido-3-oxobenzo-[*d*]isothiazol-2(3*H*)-yl)methyl)-1*H*-1,2,3-triazol-1-yl)acetamide (3b):** Off White solid, Yield: 88%, m.p.: 208 °C, R_f =

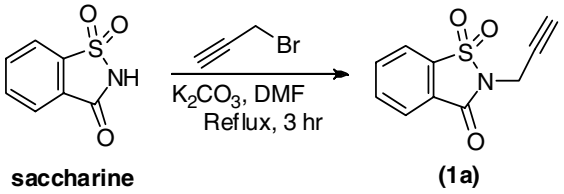

saccharine **(1a)**

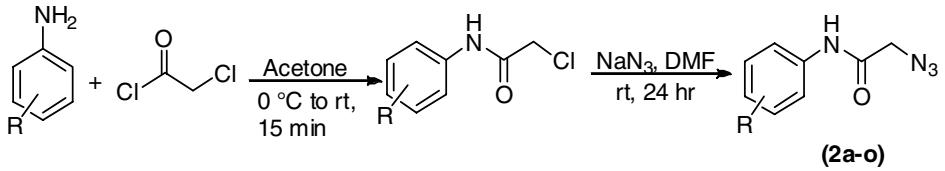

(2a-o)

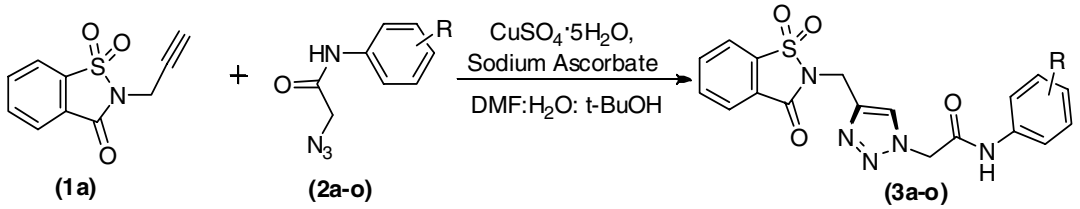

(1a) **(2a-o)** **(3a-o)**

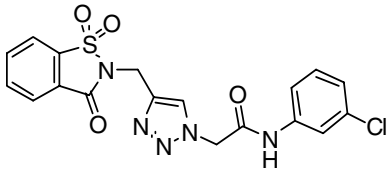

(3a), 85%

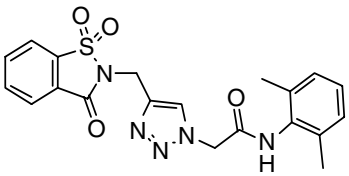

(3b), 88%

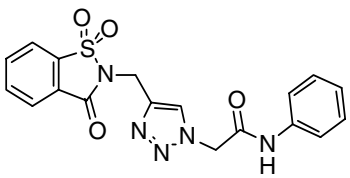

(3c), 90%

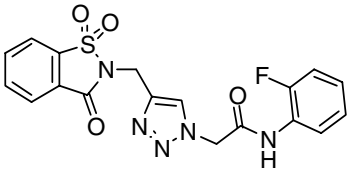

(3d), 86%

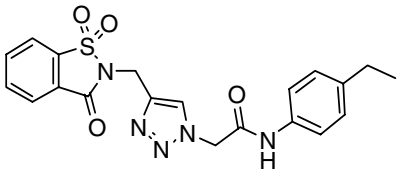

(3e), 84%

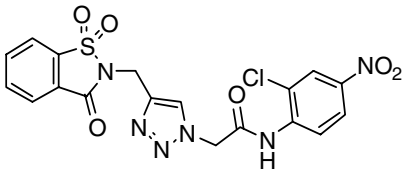

(3f), 87%

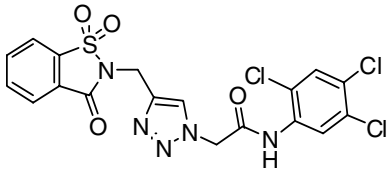

(3g), 92%

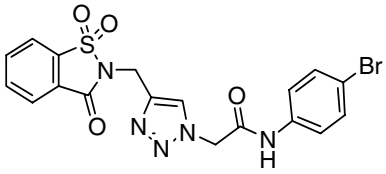

(3h), 91%

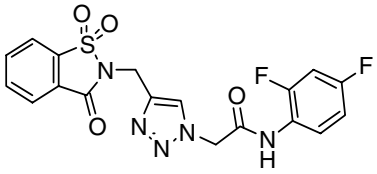

(3i), 85%

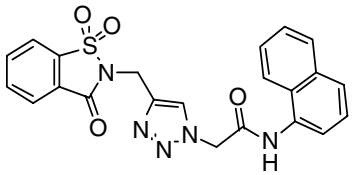

(3j), 88%

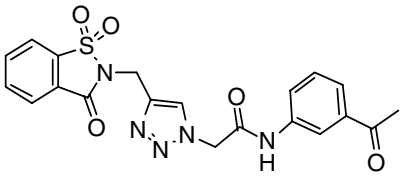

(3k), 87%

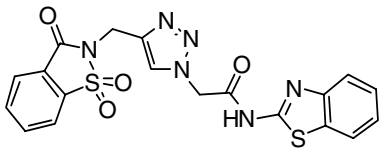

(3l), 93%

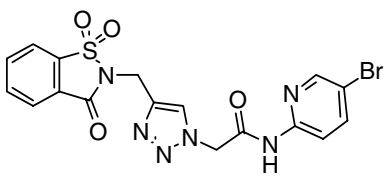

(3m), 91%,

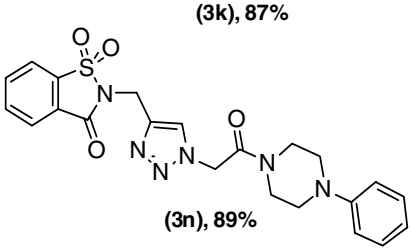

(3n), 89%

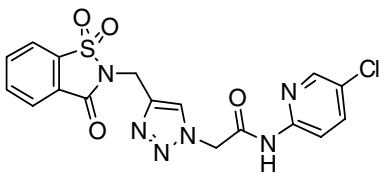

(3o), 90%

Scheme-I: Synthetic route for compounds (**3a-o**)

0.57, (10:90; MeOH:$CHCl_3$), ^{1}H NMR (400 MHz, DMSO-d_6) δ ppm: 9.42 (s, 1H), 8.10 (s, 1H), 8.03 (ddd, *J* = 7.1, 5.4, 1.5 Hz, 2H), 7.91 (td, *J* = 7.5, 1.4 Hz, 1H), 7.49 (td, *J* = 7.5, 1.5 Hz, 1H), 7.09-7.01 (m, 2H), 7.01-6.97 (m, 1H), 5.12 (s, 2H), 4.83 (d, *J* = 15.4 Hz, 1H), 4.47 (d, *J* = 15.2 Hz, 1H), 2.20 (s, 6H). ^{13}C NMR (100 MHz, DMSO) δ ppm: 163.88, 158.26, 136.82, 135.93, 135.32, 135.03, 134.13, 126.71, 126.16, 125.54, 125.16, 121.64, 51.62, 17.97. Mass (EI) calcd. for $C_{20}H_{19}N_5O_4S$ $[M+1]^+$ 425.56; found 425.02. IR (KBr, ν_{max}, cm^{-1}): 3230, 1853, 1708, 1678, 1602, 1548, 1489, 1404, 1294, 1224, 1195, 1149, 1112, 1091, 1055, 985, 887, 827, 752, 682.

2-(4-((1,1-Dioxido-3-oxobenzo[*d*]isothiazol-2(3*H*)-yl)-methyl)-1*H*-1,2,3-triazol-1-yl)-*N*-phenylacetamide (3c): Off White solid, Yield: 90%, m.p.: 224 °C, R_f = 0.71, (10:90; MeOH:$CHCl_3$), ^{1}H NMR (400 MHz, DMSO-d_6) δ ppm: 10.29 (s, 1H), 8.10 (s, 1H), 8.02 (dt, *J* = 7.6, 1.3 Hz, 2H), 7.91 (td, *J* = 7.4, 1.3 Hz, 1H), 7.63 – 7.55 (m, 2H), 7.46 (td, *J* = 7.5, 1.5 Hz, 1H), 7.35 – 7.25 (m, 2H), 7.04 (td, *J* = 7.5, 1.5 Hz, 1H), 5.14 (s, 2H), 4.83 (d, *J* = 15.4 Hz, 1H), 4.47 (d, *J* = 15.2 Hz, 1H). ^{13}C NMR (100 MHz, DMSO) δ ppm: 164.04, 158.27, 141.04, 138.35, 136.82, 135.92, 135.30, 128.87, 126.16, 125.68, 125.26, 125.16, 123.72, 121.63, 119.13, 52.18, 33.47. Mass (EI) calcd. for $C_{18}H_{15}N_5O_4S$ $[M+H]^+$ 397.08; found 397. IR (KBr, ν_{max}, cm^{-1}): 3242, 3055, 1743, 1660, 1628, 1541, 1452, 1415, 1377, 1302, 1227, 1148, 976, 902, 821, 752.

2-(4-((1,1-Dioxido-3-oxobenzo[*d*]isothiazol-2(3*H*)-yl)-methyl)-1*H*-1,2,3-triazol-1-yl)-*N*-(2-fluorophenyl)-acetamide (3d): White solid, Yield: 86%, m.p.: 242 °C, R_f = 0.60, (10:90; MeOH:$CHCl_3$), ^{1}H NMR (400 MHz, DMSO-d_6) δ 9.63 (s, 1H), 8.09 (s, 1H), 8.02 (ddd, *J* = 9.7, 7.0, 2.4 Hz, 3H), 7.91 (td, *J* = 7.4, 1.3 Hz, 1H), 7.47 (td, *J* = 7.5, 1.5 Hz, 1H), 7.21-7.04 (m, 3H), 5.12 (s, 2H), 4.83 (d, *J* = 15.4 Hz, 1H), 4.47 (d, *J* = 15.2 Hz, 1H). ^{13}C NMR (100 MHz, DMSO) δ 164.66, 158.26, 154.58, 152.15, 136.82, 126.16, 125.74, 125.66, 125.58, 125.46, 125.35, 125.17, 124.48, 123.65, 121.64, 115.66, 115.47, 51.97, 33.45. Mass (EI) calcd. for $C_{18}H_{14}N_5O_4SF$ $[M+1]^+$ 415.40; found 415. IR (KBr, ν_{max}, cm^{-1}): 3330, 3136, 3082, 1715, 1686, 1607, 1547, 1493, 1402, 1298, 1253, 1160, 1055, 986, 891, 829, 754.

2-(4-((1,1-Dioxido-3-oxobenzo[*d*]isothiazol-2(3*H*)-yl)methyl)-1*H*-1,2,3-triazol-1-yl)-*N*-(4-thylphenyl)acetamide (3e): Off White solid, Yield: 84%, m.p.: 184 °C, R_f = 0.61, (10:90; MeOH:$CHCl_3$), ^{1}H NMR (400 MHz, DMSO-d_6) δ ppm: 10.31 (s, 1H), 8.10 (s, 1H), 8.03 (ddd, *J* = 7.1, 5.4, 1.5 Hz, 2H), 7.91 (td, *J* = 7.5, 1.4 Hz, 1H), 7.53 – 7.43 (m, 3H), 7.12 (dt, *J* = 7.5, 1.0 Hz, 2H), 5.12 (s, 2H), 4.83 (d, *J* = 15.4 Hz, 1H), 4.47 (d, *J* = 15.2 Hz, 1H), 2.63 (qt, *J* = 8.1, 1.1 Hz, 2H), 1.21 (t, *J* = 8.0 Hz, 3H). ^{13}C NMR (100 MHz, DMSO) δ ppm: 168.43, 159.09, 141.39, 140.68, 138.94, 138.58, 133.42, 133.34, 132.90, 127.81, 125.95, 123.83, 122.11, 120.28, 120.27, 52.53, 38.86, 28.56, 15.48. Mass (EI) calcd. for $C_{20}H_{19}N_5O_4S$ $[M+1]^+$ 425.6; found 425.03. IR (KBr, ν_{max}, cm^{-1}): 3306, 3130, 3080, 1703, 1678, 1601, 1550, 1485, 1444, 1396, 1294, 1147, 1114, 1058, 985, 875, 854, 756, 684.

***N*-(2-Chloro-4-nitrophenyl)-2-(4-((1,1-dioxido-3-oxobenzo[*d*]isothiazol-2(3*H*)-yl)methyl)-1*H*-1,2,3-triazol-1-yl)acetamide (3f)**: Off White solid, Yield: 87%, m.p.: 224 °C, R_f = 0.57, (10:90; MeOH:$CHCl_3$), ^{1}H NMR (400 MHz, DMSO-d_6) δ ppm: 9.65 (s, 1H), 8.27 (d, *J* = 1.6 Hz, 1H), 8.22 (dd, *J* = 7.5, 1.5 Hz, 1H), 8.10 (s, 1H), 8.03 (dt, *J* = 7.4, 1.5 Hz, 2H), 7.97 (d, *J* = 7.5 Hz, 1H), 7.91 (td, *J* = 7.5, 1.4 Hz, 1H), 7.63 (td, *J* = 7.6, 1.5 Hz, 1H), 5.13 (s, 2H), 4.84 (s, 2H). ^{13}C NMR (100 MHz, DMSO) δ ppm: 168.39, 159.14, 141.38, 140.76, 139.36, 138.47, 133.70, 133.33, 132.85, 126.12, 125.69, 124.88, 124.43, 124.09, 122.10, 122.07, 52.53, 37.82. Mass (EI) calcd. for $C_{18}H_{13}N_6O_6SCl$ [M+H]+ 476.85; found 476. IR (KBr, ν_{max}, cm^{-1}): 3330, 3140, 3085, 1708, 1678, 1608, 1550, 1510, 1481, 1408, 1296, 1261, 1217, 1149, 1053, 985, 831, 752, 682.

2-(4-((1,1-Dioxido-3-oxobenzo[*d*]isothiazol-2(3*H*)-yl)methyl)-1*H*-1,2,3-triazol-1-yl)-*N*-(2,4,5-trichlorophenyl)-acetamide (3g): Off White solid, Yield: 92%, m.p.: 236 °C, R_f = 0.50, (10:90; MeOH:$CHCl_3$), ^{1}H NMR (400 MHz, DMSO-d_6) δ ppm: 9.56 (s, 1H), 8.10 (s, 1H), 8.03 (dt, *J* = 7.4, 1.6 Hz, 2H), 7.96 (s, 1H), 7.91 (td, *J* = 7.5, 1.4 Hz, 1H), 7.74 (s, 1H), 7.46 (td, *J* = 7.6, 1.5 Hz, 1H), 5.13 (s, 2H), 4.84 (s, 2H). ^{13}C NMR (100 MHz, DMSO) δ ppm: 168.33, 159.14, 141.38, 138.50, 135.62, 133.58, 133.11, 132.76, 130.51, 129.26, 127.90, 126.12, 125.68, 124.08, 122.10, 121.08, 52.50, 38.22. Mass (EI) calcd. for $C_{18}H_{12}N_5O_4S$ Cl_3 $[M+H]^+$ 500; found 501. IR (KBr, ν_{max}, cm^{-1}): 3315, 3112, 3095, 1703, 1624, 1554, 1529, 1458, 1352, 1265, 1159, 1051, 977, 889, 842, 804.

***N*-(4-Bromophenyl)-2-(4-((1,1-dioxido-3-oxobenzo[*d*]-isothiazol-2(3*H*)-yl)methyl)-1*H*-1,2,3-triazol-1-yl)acetamide (3h)** Off White solid, Yield: 91%, m.p.: 226 °C, R_f = 0.65, (10:90; MeOH:$CHCl_3$), ^{1}H NMR (400 MHz, DMSO-d_6) δ ppm: 10.36 (s, 1H), 8.10 (s, 1H), 8.03 (ddd, *J* = 7.4, 5.9, 1.6 Hz, 2H), 7.91 (td, *J* = 7.5, 1.5 Hz, 1H), 7.60-7.53 (m, 2H), 7.53-7.45 (m, 2H), 7.44 (d, *J* = 1.3 Hz, 1H), 5.15 (s, 2H), 4.84 (s, 2H). ^{13}C NMR (100 MHz, DMSO) δ ppm: 168.74, 159.10, 141.38, 139.61, 138.47, 133.70, 133.25, 132.85, 131.67, 131.58, 126.04, 124.03, 122.10, 121.96, 118.06, 52.53, 38.17. Mass (EI) calcd. for $C_{18}H_{14}N_5O_4SBr$ $[M+2]^+$ 476; found 478. IR (KBr, ν_{max}, cm^{-1}): 3330, 3130, 3080, 1710, 1676, 1600, 1533, 1481, 1390, 1296, 1224, 1197, 1147, 1111, 1053, 981, 885, 817, 852, 678.

***N*-(2,4-Difluorophenyl)-2-(4-((1,1-dioxido-3-oxobenzo-[*d*]isothiazol-2(3*H*)-yl)methyl)-1*H*-1,2,3-triazol-1-yl)-acetamide (3i):** Off White solid, Yield: 85%, m.p.: 244 °C, R_f = 0.59, (10:90; MeOH:$CHCl_3$), ^{1}H NMR (400 MHz, DMSO-d_6) δ ppm: 9.63 (s, 1H), 8.09 (s, 1H), 8.03 (ddd, *J* = 7.1, 5.3, 1.5 Hz, 2H), 7.91 (td, *J* = 7.5, 1.4 Hz, 1H), 7.78 (dt, *J* = 7.5, 5.0 Hz, 1H), 7.54 (td, *J* = 7.5, 1.5 Hz, 1H), 7.11 (td, *J* = 8.0, 1.5 Hz, 1H), 7.03 (td, *J* = 7.7, 1.4 Hz, 1H), 5.12 (s, 2H), 4.83 (d, *J* = 15.4 Hz, 1H), 4.47 (d, *J* = 15.2 Hz, 1H). ^{13}C NMR (100 MHz, DMSO) δ ppm: 168.41, 159.09, 156.39, 153.64, 141.39, 138.47, 133.42, 133.34, 132.90, 126.05, 123.93, 122.08, 122.05, 112.39, 105.47, 52.51, 38.82168.41, 159.09, 156.39, 153.64, 141.39, 138.47, 133.42, 133.34, 132.90, 126.05, 123.93, 122.08, 122.05, 112.39, 105.47, 52.51, 38.82. Mass (EI) calcd. for $C_{18}H_{13}N_5O_4SF_2$ $[M+2]^+$ 433; found 435. IR (KBr, ν_{max}, cm^{-1}): 3310, 3130, 3022, 1710, 1678, 1546, 1485, 1456, 1394, 1298, 1255, 1232, 1199, 1149, 1114, 1053, 1010, 977, 889, 815, 752, 680.

2-(4-((1,1-Dioxido-3-oxobenzo[*d*]isothiazol-2(3*H*)-yl)methyl)-1*H*-1,2,3-triazol-1-yl)-*N*-(naphthalen-1-yl)-

acetamide (3j): Off White solid, Yield: 88%, m.p.: 182 °C, R_f = 0.74, (10:90; MeOH:$CHCl_3$), ^{1}H NMR (400 MHz, DMSO-d_6) δ ppm: 9.82 (s, 1H), 8.09 (d, *J* = 8.7 Hz, 2H), 8.03 (td, *J* = 7.9, 1.5 Hz, 2H), 7.91 (td, *J* = 7.5, 1.5 Hz, 1H), 7.83 (dt, *J* = 7.1, 1.7 Hz, 1H), 7.73 (dt, *J* = 7.4, 1.5 Hz, 1H), 7.63 (ddd, *J* = 7.6, 3.8, 1.6 Hz, 2H), 7.59-7.41 (m, 3H), 5.13 (s, 2H), 4.83 (d, *J* = 15.4 Hz, 1H), 4.47 (d, *J* = 15.2 Hz, 1H). ^{13}C NMR (100 MHz, DMSO) δ ppm: 168.53, 159.14, 141.39, 138.47, 136.90, 134.48, 133.70, 133.33, 132.84, 127.00, 126.92, 126.35, 126.13, 125.70, 125.63, 125.20, 123.95, 122.08, 52.55, 38.52. Mass (EI) calcd. for $C_{22}H_{17}N_5O_4S$ $[M+1]^+$ 447; found 447. IR (KBr, ν_{max}, cm^{-1}): 3329, 3138, 3082, 2129, 1708, 1678, 1600, 1548, 1481, 1444, 1390, 1292, 1224, 1197, 1143, 1112, 1053, 754, 680.

***N*-(3-Acetylphenyl)-2-(4-((1,1-dioxido-3-oxobenzo[*d*]-isothiazol-2(3*H*)-yl)methyl)-1*H*-1,2,3-triazol-1-yl)acetamide (3k):** Off White solid, Yield: 87%, m.p.: 232 °C, R_f = 0.70, (10:90; MeOH:$CHCl_3$), ^{1}H NMR (400 MHz, DMSO-d_6) δ ppm: 10.22 (s, 1H), 8.14 (t, *J* = 1.5 Hz, 1H), 8.10 (s, 1H), 8.03 (ddd, *J* = 7.3, 5.4, 1.5 Hz, 2H), 7.91 (td, *J* = 7.5, 1.5 Hz, 1H), 7.76 (dt, *J* = 7.5, 1.5 Hz, 1H), 7.65 (dt, *J* = 7.5, 1.5 Hz, 1H), 7.54 (td, *J* = 7.5, 1.5 Hz, 1H), 7.43 (t, *J* = 7.5 Hz, 1H), 5.12 (s, 2H), 4.83 (d, *J* = 15.4 Hz, 1H), 4.47 (d, *J* = 15.2 Hz, 1H), 2.57 (s, 3H). ^{13}C NMR (100 MHz, DMSO) δ ppm: 197.10, 168.58, 159.10, 141.39, 139.18, 138.96, 138.47, 133.37, 133.35, 132.85, 128.20, 126.04, 124.02, 123.33, 122.07, 121.75, 117.74, 52.56, 38.82, 26.48. Mass (EI) calcd. for $C_{20}H_{17}N_5O_5S$ $[M+H]^+$ 439.2; found 440. IR (KBr, ν_{max}, cm^{-1}): 3330, 3132, 3080, 1919, 1907, 1870, 1826, 1770, 1716, 1683, 1622, 1510, 1458, 1357, 1300, 1153, 1078, 1055, 877, 750, 670.

***N*-(Benzo[*d*]thiazol-2-yl)-2-(4-((1,1-dioxido-3-oxobenzo-[*d*]isothiazol-2(3*H*)-yl)methyl)-1*H*-1,2,3-triazol-1-yl)-acetamide (3l):** Off White solid, Yield: 93%, m.p.: 230 °C, R_f = 0.60, (10:90; MeOH:$CHCl_3$), ^{1}H NMR (400 MHz, DMSO-d_6) δ ppm: 10.51 (s, 1H), 8.26 (d, *J* = 1.4 Hz, 1H), 8.11-7.99 (m, 4H), 7.95-7.83 (m, 2H), 7.49 (td, *J* = 7.5, 1.5 Hz, 1H), 5.14 (s, 2H), 4.84 (s, 2H). ^{13}C NMR (100 MHz, DMSO) δ ppm: 169.28, 159.10, 150.92, 148.66, 141.34, 139.63, 138.47, 133.70, 133.25, 132.85, 126.04, 124.09, 122.13, 115.24, 112.75, 52.45, 38.13. Mass (EI) calcd. for $C_{19}H_{14}N_6O_4S_2$ $[M+H]^+$ 454; found 454. IR (KBr, ν_{max}, cm^{-1}): 3310, 3125, 3085, 1700, 1624, 1554, 1532, 1460, 1350, 1260, 1160, 1050, 980, 890, 845, 805.

***N*-(5-Bromopyridin-2-yl)-2-(4-((1,1-dioxido-3-oxobenzo-[*d*]isothiazol-2(3*H*)-yl)methyl)-1*H*-1,2,3-triazol-1-yl)-acetamide (3m):** Off White solid, Yield: 91%, m.p.: 204 °C, R_f = 0.53, (10:90; MeOH:$CHCl_3$), ^{1}H NMR (400 MHz, DMSO-d_6) δ ppm: 10.45 (s, 1H), 8.38 (d, *J* = 4.2 Hz, 1H), 8.22 (s, 1H), 7.72-7.52 (m, 2H), 7.43 (d, *J* = 10.2 Hz, 2H), 7.40-7.24 (m, 3H), 5.61 (s, 2H), 5.27 (s, 2H). ^{13}C NMR (100 MHz, DMSO) δ ppm: 165.82, 156.49, 156.36, 149.29, 149.18, 143.60, 142.54, 128.89, 128.60, 127.12, 125.09, 124.85, 124.80, 123.84, 123.25, 115.80, 115.75, 114.94, 62.02, 52.34. Mass (EI) calcd. for $C_{17}H_{13}BrN_6O_4S$ $[M+2]^+$ 475; found 477. IR (KBr, ν_{max}, cm^{-1}): 3316, 3130, 3096, 1919, 1843, 1793, 1718, 1681, 1620, 1554, 1519, 1456, 1417, 1340, 1301, 1186, 1151, 1055, 894, 752, 670.

2-((1-(2-Oxo-2-(4-phenylpiperazin-1-yl)ethyl)-1*H*-1,2,3-triazol-4-yl)methyl)benzo[*d*]isothiazol-3(2*H*)-one 1,1-dioxide (3n): Off White solid, Yield: 89%, m.p.: 222 °C, R_f = 0.60, (10:90; MeOH:$CHCl_3$), ^{1}H NMR (400 MHz, DMSO-d_6) δ ppm: 8.11 (s, 1H), 8.03 (ddd, *J* = 7.3, 5.5, 1.5 Hz, 2H), 7.90 (td, *J* = 7.5, 1.5 Hz, 1H), 7.65 (td, *J* = 7.5, 1.5 Hz, 1H), 7.26-7.17 (m, 2H), 6.97-6.89 (m, 2H), 6.82 (dd, *J* = 7.5, 1.5 Hz, 1H), 5.15 (s, 2H), 4.84 (d, *J* = 15.2 Hz, 1H), 4.49 (d, *J* = 15.2 Hz, 1H), 3.66-3.58 (m, 4H), 3.46-3.38 (m, 4H). ^{13}C NMR (100 MHz, DMSO) δ ppm: 169.84, 159.14, 150.57, 141.34, 138.47, 133.72, 133.34, 133.17, 129.20, 126.12, 124.14, 121.88, 118.10, 116.32, 116.23, 52.06, 48.09, 48.04, 44.88, 44.86, 37.78. Mass (EI) calcd. for $C_{22}H_{12}N_6O_4S$ $[M+H]^+$ 466; found 466. IR (KBr, ν_{max}, cm^{-1}): 3310, 3125, 3089, 1919, 1716, 1685, 1622, 1554, 1512, 1458, 1415, 1359, 1298, 1147, 1078, 1055, 983, 877, 752, 670.

***N*-(5-Chloropyridin-2-yl)-2-(4-((1,1-dioxido-3-oxo-benzo[*d*]isothiazol-2(3*H*)-yl)methyl)-1*H*-1,2,3-triazol-1-yl)acetamide (3o):** Off White solid, Yield: 90%, m.p.: 242 °C, R_f = 0.65, (10:90; MeOH:$CHCl_3$), ^{1}H NMR (400 MHz, DMSO-d_6) δ ppm: 10.51 (s, 1H), 8.19 (d, *J* = 1.6 Hz, 1H), 8.09 (s, 1H), 8.07-7.99 (m, 3H), 7.91 (td, *J* = 7.5, 1.4 Hz, 1H), 7.81 (dd, *J* = 7.5, 1.5 Hz, 1H), 7.52 (td, *J* = 7.5, 1.5 Hz, 1H), 5.13 (s, 2H), 4.83 (d, *J* = 15.4 Hz, 1H), 4.47 (d, *J* = 15.2 Hz, 1H). ^{13}C NMR (100 MHz, DMSO) δ ppm: 169.28, 159.06, 150.89, 147.03, 141.39, 138.47, 137.79, 133.42, 133.32, 132.90, 126.12, 125.77, 123.94, 122.13, 115.23, 52.48, 38.86. Mass (EI) calcd. for $C_{17}H_{13}N_5O_4SCl$ $[M+2]^{l+}$ 432; found 434. IR (KBr, ν_{max}, cm^{-1}): 3257, 3136, 3093, 1718, 1685, 1640, 1626, 1585, 1525, 1494, 1460, 1365, 1327, 1303, 1155, 976, 754.

Molecular docking: The level of anticancer activities demonstrated by the compounds against the breast cancer cell lines prompted us to perform molecular docking studies to understand their plausible mechanism of action and gain an insight into ligand-protein interactions. All the calculations were performed using Glide (Grid-Based Ligand Docking with Energetics) program [23,24] integrated in the Schrödinger molecular modeling package (Schrödinger, LLC, New York, 2018). With this purpose, the crystal structure of Epidermal Growth Factor Receptor Tyrosine Kinase, a crucial target intervening the cancer pathophysiology, was retrieved from the protein data bank (PDB) (pdb code: 1M17) and refined using the protein preparation wizard. The 3D structures of compounds to be docked were sketched using the build panel in Maestro and optimized using the Ligand Preparation tool. Both the enzyme as well as ligand structures were subjected to energy minimization until their average RMSD of heavy atoms reached 0.01 Å. The active site of enzyme was defined the receptor grid generation panel to include residues within a 12.0 Å radius of co-crystallized ligand in the crystal complex. With this setup, flexible docking was executed against the EGFR Tyrosine Kinase using with extra precision (*i.e.* with GlideXP) scoring function to identify the binding modes and affinities towards the target. The output files *i.e.* the docking poses were visualized and then quantitatively analyzed for the most significant thermodynamic elements of interactions with the active site residues using the Maestro′s Pose Viewer utility.

RESULTS AND DISCUSSION

Firstly, 2-(prop-2-yn-1-yl)benzo[*d*]isothiazol-3(2*H*)-one 1,1-dioxide (**1a**) was synthesized by the reaction of saccharine

with propargyl bromide in the presence of K_2CO_3 at reflux temperature in DMF. 2-Azido-*N*-substituted phenylacetamide was synthesized by a reaction between 2-chloro-*N*-substituted phenylacetamide and sodium azide in DMF. In this report $CuSO_4$ has been considered as a best catalyst along with sodium ascorbate. Sodium ascorbate play a dual role, it act as a ligand and reducing agent. It was observed that without the use of reducing agent reaction was not progressed. (Table-1, entry 1). The solvent solvent conditions were also optimized and DMF + *t*-BuOH + water with (2:1:2) ratio gets a highest yield (Table-1, entry 2). For further investigations, the reaction methodology against various amine substrate were also checked and the reaction was successfully conducted without the any problem. All substrates were sufficient pure and had a moderate yield.

All 1,2,3-triazol-saccharine hybrids (**3a-o**) were well characterized by ^1H & ^{13}C NMR analysis. In compounds **3a-o**, ^1H NMR analysis showed one NH signal (labile with D_2O), which was observed at 9.42-10.50 δ ppm. In ^{13}C NMR, amide and cyclic amide, signals were observed at 164.66 and 156.50 δ ppm, respectively. With more analytical analysis, all compounds showed a proposed mass in their mass-ESI data. IR analysis showed a broad band NH stretching at 3300-3200 cm^{-1} and C=O stretching at 1710-1650 cm^{-1} range.

Proposed reaction mechanism: Proposed reaction mechanism stated that copper(II) was reduced into copper(I) sodium ascorbate, it also worked as a ligand and made adduct with **b** convert into **c**. Then intermediate **c** spontaneously reacted with **d** to form intermediate **e**. A intermolecular [3+2] cycloaddition took place and converted into intermediate **h** *via* **g** and **f**, finally ligand and Cu(I) eliminated and goes to next cycles (Fig. 2).

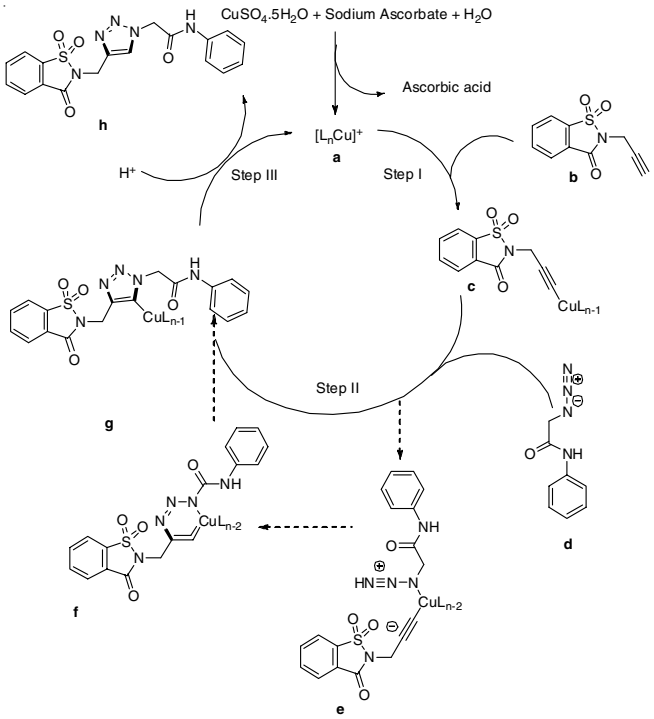

Fig. 2. Proposed reaction mechanism

TABLE-1
OPTIMIZATION OF COPPER CATALYZED CLICK CHEMISTRY

Entry	Solvent	Catalyst	Reducing agent	Yield (%)
1	DMF + *t*-BuOH + water (2:1:2)	$CuSO_4·5H_2O$	–	Traces
2	DMF + *t*-BuOH + water (2:1:2)	$CuSO_4·5H_2O$	Sodium ascorbate	93
3	DMF + *t*-BuOH + water (2:1:2)	$Cu(OAc)_2$	Sodium ascorbate	86
4	DMF + *t*-BuOH + water (2:1:2)	$Cu(OAc)_2$	–	Traces
5	DMF + *t*-BuOH + water (1:1:1)	$CuSO_4·5H_2O$	Sodium ascorbate	82
6	*t*-BuOH	$CuSO_4·5H_2O$	Sodium ascorbate	42
7	DMF	$CuSO_4·5H_2O$	Sodium ascorbate	86

Reaction condition: Starting materials 3-(prop-2-yn-1-yloxy)-2*H*-chromen-2-one (1 mmol), **2a** (1 mmol), 0.2 equiv. of appropriate Cu-Sources, reducing agent and solvent.

TABLE-2
MOLECULAR DOCKING ENERGY AND BINDING AFFINITY

Compd.	Breast cancer (Growth %)						Molecular docking		
	MCF7	MDA-MB-231/ATCC	HS 578T	BT-549	T-47D	MDA-MB-468	Glide score	Glide energy	H-Bond
3a	92.45	114.52	106.69	132.51	96.98	100.50	-7.739	-44.217	Cys773 (1.84), Asp831 (1.75)
3b	97.40	112.62	95.31	111.97	97.68	100.24	-7.108	-39.051	Met769 (2.03), Asp831 (1.66)
3c	91.79	105.12	88.33	106.61	91.24	104.41	-7.846	-45.564	Cys773 (2.15), Asp831 (1.74)
3d	97.77	104.59	93.91	105.37	92.78	97.06	-7.101	-38.210	Cys773 (2.36), Asp831 (2.19)
3e	86.55	90.93	87.73	98.37	81.43	107.42	-8.16	-48.538	Cys773 (2.29), Asp831 (1.99)
3f	83.04	90.04	92.91	102.89	76.94	102.96	-8.33	-50.019	Cys773 (2.57), Asp831 (2.12)
3g	86.67	92.28	97.50	99.67	81.12	106.30	-8.05	-47.272	Met769 (2.18), Asp831 (1.76)
3h	89.20	85.13	83.96	98.57	82.38	107.11	-7.998	-46.834	Cys773 (2.02), Asp831 (1.77)
3i	91.20	101.66	98.07	97.80	89.50	100.08	-7.823	-45.332	Cys773 (2.36), Asp831 (2.15)
3j	93.50	99.33	91.25	101.00	90.01	104.19	-7.315	-42.180	Asp831 (2.39)
3k	91.11	84.26	115.88	101.29	89.47	118.81	-7.554	-45.493	Cys773 (2.43), Asp831 (1.72)
3l	91.14	107.89	109.68	97.86	88.13	130.48	-7.426	-45.419	Cys773 (2.33), Asp831 (1.77)
3m	88.32	108.61	110.65	97.49	89.32	120.13	-8.01	-47.096	Cys773 (2.46), Asp831 (1.70)
3n	94.42	100.42	86.17	99.23	107.34	110.76	-7.196	-40.752	–
3o	93.88	102.64	96.77	109.36	103.11	100.88	-7.222	-41.873	Cys773 (2.45), Asp831 (1.71)

Molecular docking: A perusal of docking output revealed that the binding affinities of the compounds corroborated well with the experimental anticancer potency showing a significant linear correlation with an average docking score of -7.658 and Glide binding energy-44.523 kcal/mol (Table-2). All the compounds could optimally fit into the active site of the enzyme adopting a very similar orientation at coordinates close to the co-crystallized ligand and the complex formed with the target enzyme was stabilized through a network of significant bonded and non-bonded interactions.

Furthermore, a quantitative analysis of pre-residue interaction between these compounds and the active site residues of the enzyme could provide an insight into the most significantly interacting residues and the type of thermodynamic interactions that govern their affinity to EGFR Tyrosine Kinase. This is elaborated for the one of the most active compound **3f** (Fig. 3).

The enzyme-inhibitor was stabilized by a network of significant van der Waals interactions observed with Leu820 (-3.151 kcal/mol), Asn818 (-1.498 kcal/mol), Arg817 (-3.707 kcal/mol), Cys773 (-3.032 kcal/mol), Gly772(-3.188 kcal/mol), Phe771 (-1.37 kcal/mol), Pro770 (-1.141 kcal/mol), Met769(-3.236 kcal/mol), Leu768 (-2.101 kcal/mol), Glu738 (-1.204 kcal/mol), Lys721 (-4.496 kcal/mol), Phe699 (-1.847 kcal/mol) and Leu694 (-4.44 kcal/mol) residues through 4-((1,1-dioxido-3-oxobenzo[*I*]isothiazol-2(3*H*)-yl)methyl)-1*H*-1,2,3-triazole component of the molecule while *N*-phenylacetamide fragment was engaged in similar type of interactions with Asp831 (-3.284 kcal/mol), Thr830 (-2.49 kcal/mol), Thr766 (-2.004 kcal/mol), Leu764 (-2.296 kcal/mol), Met 742(-1.824 kcal/mol), Ala719 (-1.436 kcal/mol) and Val702 (-2.347 kcal/mol) lining the active site. These steric interactions were further complimented by a significant electrostatic interaction as well observed with Asp831 (-10.551 kcal/mol), Asn818 (-1.581 kcal/mol), Asp813 (-1.134 kcal/mol), Met769 (-1.31 kcal/mol), Glu738 (-4.259 kcal/mol) and Lys690 (-1.327 kcal/mol) residues in the active site. While these non-bonded interactions were observed to be principle driving force for anchoring compound **3f** into active site, a high binding affinity observed was also attributed to two prominent hydrogen bonding interactions: firstly with Cys773 through the oxo function (O=S=O) and secondly with Asp831 through amide (-NH-) function having a bond distance of 2.57 and 2.12 Å, respectively. Such hydrogen bonding interactions serve as an anchor for guiding the orientation of ligand in the 3D space of active site and facilitate the other non-bonded interactions adding to the stability of enzyme-inhibitor complex. Similar set of bonded and non-bonded interactions were involved in stabilizing the complexes of other molecules in the series. Thus, the per-residue ligand interaction analysis indicates that steric complementarity between these ligands and the active site residues of Tyrosine Kinase is the primary driving forces for mechanical interlocking which was evident from the relatively higher contribution of van der Waals interactions than the other interactions responsible for the binding affinity. This information could be fruitfully utilized for the point specific mutation around the scaffold to identify potent and selective Tyrosine Kinase inhibitors.

Anti-cancer screening: Newly synthesized triazole derivatives were evaluated for anti-cancer screening at National Cancer Institute-NCI, USA. The tested cell-lines panel having total 60 various human cancer cell-lines are as leukemia cell line, non-small cell lung cancer cell-lines, colon cancer cell-lines, CNS cancer cell-lines, melanoma cell-lines, ovarian cancer cell-lines, renal cancer cell-lines. All mentioned cancer cell-line panels were divided into their individual sub-cell lines. *in-vitro* examine results of the preliminary single dose (10 µM) screening of NSC D-800361/1, NSC D-800363/1, NSC D-800364/1, NSC D-800365/1, NSC D-800366/1, NSC D-800367/1, NSC D-800368/1, NSC D-800369/1, NSC D-800370/1, NSC D-801788/1 and NSC D-801789/1 against the 60 cell lines as one dose mean graphs results of the percent growth of treated compounds are summarized in Table-3.

On the basis of anti-cancer screening one dose response graph, it is defensible that the most of the compounds (**3a**, **3c**, **3d**, **3e**, **3f**, **3g**, **3i**, **3j** and **3l**) have higher GI_{50} values against SK-OV-3 (ovarian cancer) cell line as compared to other tested cell lines. Hybrid **3j** exhibited more significant cytotoxic activity among all the tested compounds (SK-OV-3; GI_{50} = 37.19). Compound **3h** shows activity against UO-31 (renal cancer) cell line with the GI_{50} = 21.27 value. Compound **3k** shows activity against SNB-75 (CNS cancer) cell line with the moderate GI_{50} = 19.73 value. Among all the compounds, compound **3l** shows moderate activity against three various cell-lines as a GI_{50} = 30.92, GI_{50} = 21.03 and GI_{50} = 18.22, respectively to UO-31 (renal cancer), SK-OV-3 (ovarian cancer) and SNB-75 (CNS cancer).

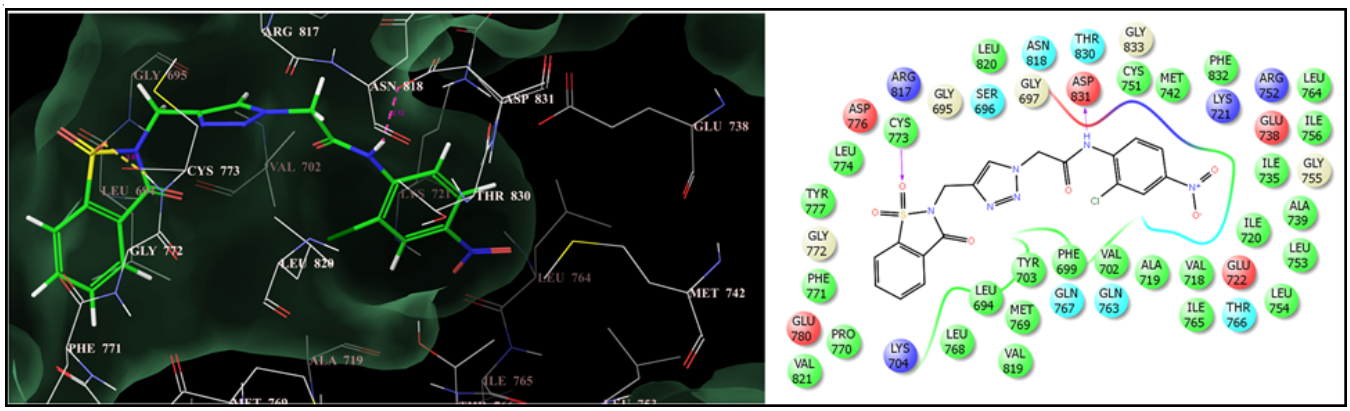

Fig. 3. Binding mode of compound **3f** into the active site of EGFR tyrosine kinase. (on right side: green lines indicate hydrogen bonding interactions)

TABLE-3
ANTICANCER SCREENING DATA OF TESTED COMPOUNDS

Compd.	NCI Code	60 Cell line assay in one dose at 10^{-5} concentration		
		Mean growth (%)	Active cell lines	Growth (%)
3a	D-800361/1	104.79	Ovarian cancer (SK-OV-3)	-20.73
3c	D-800363/1	99.11	Ovarian cancer (SK-OV-3)	-19.28
3d	D-800364/1	99.96	Ovarian cancer (SK-OV-3)	-21.89
3e	D-800365/1	97.99	Ovarian cancer (SK-OV-3)	-23.80
3f	D-800366/1	98.38	Ovarian cancer (SK-OV-3)	-26.54
3g	D-800367/1	97.85	Ovarian cancer (SK-OV-3)	-25.78
3h	D-800368/1	95.69	Renal cancer (UO-31)	-21.27
3i	D-800369/1	98.48	Ovarian cancer (SK-OV-3)	-24.04
3j	D-800370/1	98.78	Ovarian cancer (SK-OV-3)	-37.19
3k	D-801788/1	100.51	CNS cancer (SNB-75)	-19.73
3l	D-801789/1	100.52	Renal cancer (UO-31)	-30.92
			Ovarian cancer (SK-OV-3)	-21.03
			CNS cancer (SNB-75)	-18.22

Conclusion

In this work, we have successfully developed a synthetic protocol for triazole derivatives by using copper(I)-catalyzed azide alkyne cycloaddition (CuAAC) click chemistry approach to prepare analogous of saccharine containing core skeletons (**3a-o**) and evaluated their potency against 60 cell line as an anticancer agent. The structure was confirmed by mass, ^{1}H & ^{13}C NMR. Molecular docking studies showed that the lowest energy conformation of compound **3f** complexed with EGFR was found to be snugly bound to the active site at the same co-ordinates as the native ligand with a significantly higher binding affinity (docking score of -8.33 and Glide binding energy -50.019 kcal/mol) engaging in a series of bonded and non-bonded interactions. Evaluation data of *in vitro* anticancer study of synthesized saccharine-triazole hybrid adducts showed that most of these compounds exhibited moderate cytotoxicity. Out of 15 compounds 9 compounds shows activity against ovarian cancer (SK-OV-3) cancer cell line while other compounds showed moderate activity against renal cancer and CNS cancer cell lines. In view of overall data, the significant results would be useful to develop new strategy for the next target with better-quality effectiveness and influence of molecules for additional therapeutic position.

ACKNOWLEDGEMENTS

The authors are highly thankful to the Department of Chemistry (UGC-SAP, FIST sponsored), Saurashtra University for laboratory facilities and National Facility for Drug Discovery Complex (NFDD) for providing instrumentation support. The authors are also thankful to the National Cancer Institute (NCI), a part of the National Institute of Health (NIH), Bethesda, U.S.A., which is an aspirant of the research on anticancer screening. One of the authors, KP is also thankful to Gujarat State Biotechnological Mission, India for a fellowship as well as financial assistance with reference letter no.: GSBTM/MD/PROJECTS/SSA/5044/2016-17.

REFERENCES

1. B. Meunier, Hybrid Molecules with a Dual Mode of Action: Dream or Reality?, *Acc. Chem. Res.*, **41**, 69 (2008); https://doi.org/10.1021/ar7000843
2. F. Himo, T. Lovell, R. Hilgraf, V.V. Rostovtsev, L. Noodleman, K.B. Sharpless and V.V. Fokin, Copper(I)-Catalyzed Synthesis of Azoles. DFT Study Predicts Unprecedented Reactivity and Intermediates, *J. Am. Chem. Soc.*, **127**, 210 (2005); https://doi.org/10.1021/ja0471525
3. A.L. Garner, cat-ELCCA: Catalyzing Drug Discovery through Click Chemistry, *Chem. Commun.*, **54**, 6531 (2018); https://doi.org/10.1039/C8CC02332H
4. P. Thirumurugan, D. Matosiuk and K. Jozwiak, Click Chemistry for Drug Development and Diverse Chemical-Biology Applications, *Chem. Rev.*, **113**, 4905 (2013); https://doi.org/10.1021/cr200409f
5. J. Huo, H. Hu, M. Zhang, X. Hu, M. Chen, D. Chen, J. Liu, G. Xiao, Y. Wang and Z. Wen, A Mini Review of the Synthesis of Poly-1,2,3-triazole-Based Functional Materials, *RSC Adv.*, **7**, 2281 (2017); https://doi.org/10.1039/C6RA27012C
6. D. Pasini, The Click Reaction as an Efficient Tool for the Construction of Macrocyclic Structures, *Molecules*, **18**, 9512 (2013); https://doi.org/10.3390/molecules18089512
7. M.-H. Hu, X. Chen, S.-B. Chen, T.-M. Ou, M. Yao, L.-Q. Gu, Z.-S. Huang and J.-H, Tan, A New Application of Click Chemistry *in situ*: Development of Fluorescent Probe for Specific G-quadruplex Topology, *Sci. Rep.*, **5**, 17202 (2015); https://doi.org/10.1038/srep17202
8. J.P. Meyer, P. Adumeau, J.S. Lewis and B.M. Zeglis, Click Chemistry and Radiochemistry: The First 10 Years, *Bioconjug. Chem.*, **27**, 2791 (2016); https://doi.org/10.1021/acs.bioconjchem.6b00561
9. B. Kahveci, F. Yilmaz, E. Mentese and S. Ülker, Design, Synthesis, and Biological Evaluation of Coumarin-Triazole Hybrid Molecules as Potential Antitumor and Pancreatic Lipase Agents, *Arch. Pharm.*, **350**, 1600369 (2017); https://doi.org/10.1002/ardp.201600369
10. M.H. Shaikh, D.D. Subhedar, F.A.K. Khan, J.N. Sangshetti and B.B. Shingate, 1,2,3-Triazole Incorporated Coumarin Derivatives as Potential Antifungal and Antioxidant Agents, *Chin. Chem. Lett.*, **27**, 295 (2016); https://doi.org/10.1016/j.cclet.2015.11.003
11. L. Han, L. Wang, X. Hou, H. Fu, W. Song, W. Tang and H. Fang, Design, synthesis and Preliminary Bioactivity Studies of 1,2-Dihydrobenzo[*d*]-isothiazol-3-one-1,1-dioxide Hydroxamic Acid Derivatives as Novel Histone Deacetylase Inhibitors, *Bioorg. Med. Chem.*, **22**, 1529 (2014); https://doi.org/10.1016/j.bmc.2014.01.045
12. M. D'Ascenzio, S. Carradori, C. De Monte, D. Secci, M. Ceruso and C.T. Supuran, Design, Synthesis and Evaluation of *N*-Substituted Saccharin Derivatives as Selective Inhibitors of Tumor-associated Carbonic Anhydrase XII, *Bioorg. Med. Chem.*, **22**, 1821 (2014); https://doi.org/10.1016/j.bmc.2014.01.056
13. M.S.A. Elsayed, M.E. El-Araby, R.A.T. Serya, A.H. El-Khatib, M.W. Linscheid and K.A.M. Abouzid, Structure-Based Design and Synthesis of Novel Pseudosaccharine Derivatives as Antiproliferative Agents and Kinase Inhibitors, *Eur. J. Med. Chem.*, **61**, 122 (2013); https://doi.org/10.1016/j.ejmech.2012.09.039

14. K.D. Combrink, H.B. Gulgeze, N.A. Meanwell, B.C. Pearce, P. Zulan, G.S. Bisacchi, D.G.M. Roberts, P. Stanley and S.M. Seiler, 1,2-Benzisothiazol-3-one 1,1-Dioxide Inhibitors of Human Mast Cell Tryptase, *J. Med. Chem.*, **41**, 4854 (1998); https://doi.org/10.1021/jm9804580
15. N. Gençer, D. Demir, F. Sonmez and M. Kucukislamoglu, New Saccharin Derivatives as Tyrosinase Inhibitors, *Bioorg. Med. Chem.*, **20**, 2811 (2012); https://doi.org/10.1016/j.bmc.2012.03.033
16. M.A. Patane, R.M. DiPardo, R.A.P. Price, R.S.L. Chang, R.W. Ransom, S.S. O'Malley, J.D. Salvo and M.G. Bock, Selective α-1A Adrenergic Receptor Antagonists. Effects of Pharmacophore Regio- and Stereochemistry on Potency and Selectivity, *Bioorg. Med. Chem. Lett.*, **8**, 2495 (1998); https://doi.org/10.1016/S0960-894X(98)00451-X
17. C.E. Sunkel, M. Fau de Casa-Juana, F.J. Cillero, J.G. Priego and M.P. Ortega, Synthesis, Platelet Aggregation Inhibitory Activity, and *in vivo* Antithrombotic Activity of New 1,4-dihydropyridines, *J. Med. Chem.*, **31**, 1886 (1988); https://doi.org/10.1021/jm00118a004
18. H. Sommermeyer, R. Schreiber, J.M. Greuel, J. De Vry and T. Glaser, Anxiolytic Effects of the 5-HT1A Receptor Agonist Ipsapirone in the Rat: Neurobiological Correlates, *Eur. J. Pharmacol.*, **240**, 29 (1993); https://doi.org/10.1016/0014-2999(93)90541-O
19. J. Blanchet, T. Macklin, P. Ang, C. Metallinos and V. Snieckus, Directed Ortho Metalation-Cross Coupling Strategies. *N*-Cumyl Arylsulfonamides. Facile Deprotection and Expedient Route to 7- and 4,7-Substituted Saccharins, *J. Org. Chem.*, **72**, 3199 (2007); https://doi.org/10.1021/jo062385v
20. M.B. Youdim and R. Ashkenazi, Serotonergic Involvement in Pharmacological Action of Anxiolytic- Sedatives Thalidomide and Supidimide, *Eur. J. Pharmacol.*, **119**, 39 (1985); https://doi.org/10.1016/0014-2999(85)90319-X
21. T. Ueda, H. Konishi and K. Manabe, Palladium-Catalyzed Reductive Carbonylation of Aryl Halides with *N*-Formylsaccharin as a CO Source, *Angew. Chem. Int. Ed.*, **52**, 8611 (2013); https://doi.org/10.1002/anie.201303926
22. T. Cochet, V. Bellosta, A. Greiner, D. Roche and J. Cossy, N-Formylsaccharin: A New Formylating Agent, *Synlett*, 1920 (2011); https://doi.org/10.1055/s-0030-1260951
23. R.A. Friesner, J.L. Banks, R.B. Murphy, T.A. Halgren, J.J. Klicic, D.T. Mainz, M.P. Repasky, E.H. Knoll, M. Shelley, J.K. Perry, D.E. Shaw, P. Francis and P.S. Shenkin, Glide: A New Approach for Rapid, Accurate Docking and Scoring. 1. Method and Assessment of Docking Accuracy, *J. Med. Chem.*, **47**, 1739 (2004); https://doi.org/10.1021/jm0306430
24. T.A. Halgren, R.B. Murphy, R.A. Friesner, H.S. Beard, L.L. Frye, W.T. Pollard and J.L. Banks, Glide: A New Approach for Rapid, Accurate Docking and Scoring. 2. Enrichment Factors in Database Screening, *J. Med. Chem.*, **47**, 1750 (2004); https://doi.org/10.1021/jm030644s